Materials Chemistry and Physics: Sustainability and Energy xxx (xxxx) 100013

Contents lists available at ScienceDirect

Materials Chemistry and Physics: Sustainability and Energy

journal homepage: www.elsevier.com

Journal logo

Eco-inspired Cu-Zn bimetallic nanoparticles for Enhanced Water Purification Technologies

Naveen Kumar Dabbeta [a], Mamtha Kante [a], Ramya Konda [a], Abhilash Devarala [a], Pranay Bhaskar Kalakonda [b], Sarvani Jowhar Khanam [c], Ramu Naidu Savu [c], Murali Banovath [c], Laxmi Srinivasa Rao Siddey [a], Vijaya Nirmala Bommaji [a], Imran Hasan [d], Parvathalu Kalakonda [a,*]

[a] *Smart Nano Materials Research Laboratory, Department of Physics, Government City PG College (A), Osmania University, Hyderabad, Telangana, 500002, India*
[b] *Department of Material Science and Engineering, North Carolina State University, Raleigh, NC, 2795, USA*
[c] *Department of Chemistry, University of Hyderabad, 500046, Hyderabad, India*
[d] *Department of Chemistry, College of Science, King Saud University, Riyadh, 11451, Saudi Arabia*

ARTICLE INFO

Keywords:
Bimetallic nanoparticles
Eco-inspired synthesis
Coffee leaf extract
Photocatalytic activity
Water purification

ABSTRACT

This study focuses on the eco-friendly synthesis of copper-zinc bimetallic nanoparticles (Cu-Zn BMNPs), using coffee plant leaf extract as a multifunctional agent for capping, reducing, and stabilizing. This approach offers a sustainable method with significant potential for photocatalytic industrial applications. The photocatalytic performance of the Cu-Zn BMNPs was evaluated in the degradation of methylene blue (MB) and rhodamine (Rh) dyes under visible light. Fourier-transform infrared spectroscopy (FTIR) was used to identify biological functional groups and phytochemical bands, while scanning electron microscopy (SEM) and X-ray diffraction (XRD) analyses provided insights into the morphological and structural characteristics of the BMNPs. UV–Vis spectroscopy reveals absorption peaks between 250 and 470 nm for Cu-Zn BMNPs, with a direct optical energy bandgap of 3.8 eV and a crystalline size of 32 nm. The Cu-Zn BMNPs achieved a degradation rate of 92.4 % for MB dye and 95.2 % for Rh dye, demonstrating their effectiveness as nano-photo-catalyst. The degradation kinetics of MB and Rd dyes were analyzed using a pseudo-first-order model. This eco-friendly synthesis reduces hazardous chemicals and uses bioactive plant compounds, offering a sustainable solution for water purification by removing toxic pollutants.

1. Introduction

The advancement in industrialization and technological development has caused tons of pollutants discharged into the water bodies ecosystem, resulting in severe environmental and health hazards [1–5]. Methylene blue (MB) and rhodamine (Rh) are widely utilized dyes across various industries, including textiles, paper, cosmetics, pharmaceuticals, and plastics [6–9]. These hazardous, cancer-causing, and persistent chemicals pose significant health risks to humans, often leading to various skin disorders [10,11]. Addressing different dye contaminants in all water bodies is both challenging and complex process. Recent research work has devised multiple approaches, including oxidation process and photo-catalysis, to clear dye pollutants effectively in water bodies [12–15]. Photocatalytic dye degradation complex process, using noble metal nanoparticles as nano-catalyst material, offers sustainable remedy for water purification [16–19]. Through this process, dye molecules are decomposed into harmless byproducts, helping to protect aquatic ecosystems. This sustainable synthesis approach highlights the significance of embracing eco-conscious industrial practices in today's mindful society.

Nanomaterials possessing a high surface area-to-volume ratio demonstrate enhanced catalytic performance and exhibit unique nonlinear optical properties [20–22]. Inorganic metal nanoparticles and their hybrid nanoparticles are highly photocatalytic under sunlight, attributed to their wide band gap (3–3.5 eV) and their ability to reduce exciton (electron-hole pair) recombination [23,24]. Cupper nanoparticles doped with zinc demonstrate strong photocatalytic activity, as copper nanoparticles effectively reduce exciton recombination rates [25,26]. The Cu-Zn BMNPs show considerable promise for dye degradation in aqueous environments due to their enhanced photocatalytic properties [27–29]. Doping ZnNPs with copper (Cu) can boost their photocatalytic response by reducing donor defect concentrations, which helps to balance their n-type conductivity [30]. The quasi one-dimensional Cu-Zn BMNPs serve as high degree of building block for

* Corresponding author.
E-mail addresses: parvathalu.k@gmail.com, parvathalu@wpi.edu (P. Kalakonda).

https://doi.org/10.1016/j.macse.2025.100013
Received 12 December 2024; Received in revised form 4 February 2025; Accepted 23 February 2025
3050-4716/© 2022

multifunctional new nanomaterials, offering a range of appealing properties [31].

The environmentally sustainable eco-inspired synthesis of BMNPs using leaf extracts has emerged as highly preferred method for eco-inspired bio-synthesis. Exploring our prior research on mono metal nanoparticles, our current work focuses on designing and development of a bio-synthesis fabrication of Cu-Zn BMNPs using a coffee leaf extract [32–37]. Coffee leaves are well known for having rich antioxidant properties which play a critical role in controlling oxidative stress levels and reducing inflammation [38]. This is novel approach and it can support immune health and improve metabolism, contributing overall wellness. Coffee plant leaves are rich in bioactive phytochemicals and biomolecules, including antioxidants, flavonoids, and polyphenols [39,40]. These phytochemicals play vital role in nanoparticles synthesis and their stability. Therefore, it would be intriguing to investigate the development or design of novel multi-metal nanoparticles using coffee leaf extract material. Next, we examine the performance of the Cu-Zn BMNPs catalyst in clearing or dye degrading process of MB and Rh dyes when exposed sunlight atmosphere. This study primarily focuses on the eco-inspired biosynthesis of Cu-Zn BMNPs and their wide range of applications in reducing water-solvable pollutants. The green synthesis method helps to improve stability and helps to control size and morphology of nanoparticles with comparing with other synthesis methods. In this work, we began investigating the photocatalytic properties of the eco-inspired Cu-Zn BMNP nanocatalyst. By evaluating the effectiveness of these BMNPs, we continue our efforts to design advanced nano-catalyst material and aimed at providing sustainable remedies for addressing water pollutants challenges. This study underscores the significance of adopting environmentally conscious the best approaches in scientific novel research.

Mono/bimetallic nanoparticles are widely regarded in environmental bionano-technology due to their unique multifunctional properties, which stem from their higher surface area-to-volume ratio. These nanomaterials possess diverse properties, including optical, electrical, catalytic, and magnetic characteristics [41–44]. Among them, Cu-Zn BMNPs demonstrate significant catalytic potential, characterized by their core-shell structures and versatile morphological properties. The effective interaction between the metal ions and extract further enhances their multifaceted properties. Interestingly, although coffee plant leaf extract has been utilized in the synthesis of BMNPs, its potential for producing Cu-Zn BMNPs has yet to be investigated. The coffee plant is well-known for its natural medicinal properties. Therefore, using coffee plant extract as a multi-functional agent for Cu-Zn BMNPs nano-catalyst synthesis and promoting it for a sustainable solution for water purification application. Photo-catalysis plays a pivotal role in research on clearing toxic contaminants in the process of water purification, significantly impacting efforts in environmental remediation [45,46,47, 49, 50, 58–66]. Fig. 1 shows illustration of waste water treatment through dye degradation process from the industries through Cu-Zn BMNPs nano-catalyst material. The significant economic influence of catalysis-driven industries, capable of generating goods worth trillions of dollars annually, underscores its global relevance [19]. Catalysis is particularly preferred in the chemical and pharmaceutical sectors due to its numerous benefits, such as ease of catalyst recovery, longevity, adaptability to continuous processes, and alignment with sustainable best practices [48]. The development of nanocatalyst nanoparticles presents significant challenges due to their structural complexities and the limited scientific knowledge about their active nucleation sites. Significant research efforts are being devoted to the development of advanced nanoparticles nano-catalysts, which are essential for achieving consistent mass production of catalyst that meets industrial requirements. Nanoparticles containing BMNPs have emerged as highly effective nano-catalysts, combining the quality, durability and scalability needed to tackle global challenges. Their distinctive characteristics and adaptability place them at the cutting edge of catalysis research, offering the

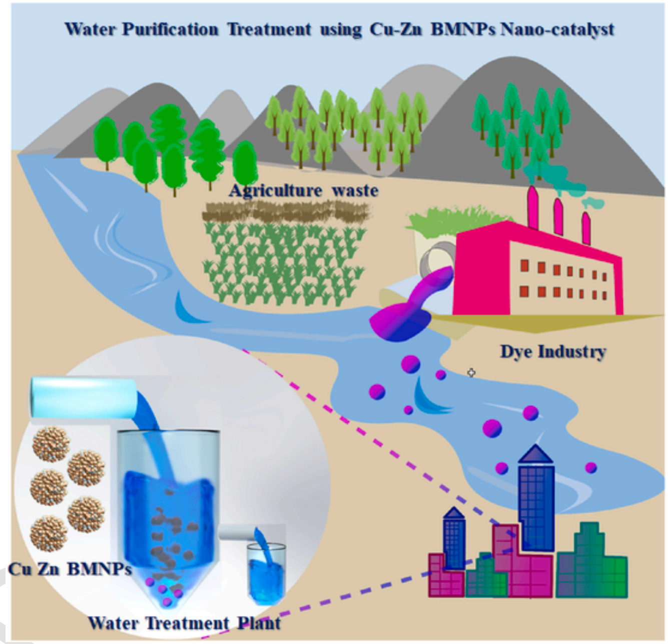

Fig. 1. Illustration of water purification through the removal of toxic elements using a nano-catalyst composed of Cu-Zn BMNPs.

potential to transform industrial processes through improved efficiency and sustainability.

This study represents an eco-inspired synthesis approach in using fresh coffee leaf extract as multifaceted agent for fabricating Cu-Zn BMNPs nano-catalyst. Our environmentally friendly synthesis method demonstrates promise for industry-scale catalyst production, underscoring its efficiency and effectiveness for sustainable water purification industrial applications. Cu-Zn BMNPs were subsequently utilized as nanocatalysts to evaluate their photocatalytic efficiency in degrading MB and Rh dyes, demonstrating excellent performance in these applications. These findings highlight the effectives of BMNPs to enhance photocatalytic processes, offering valuable prospects for environmental and waste water treatment, for the sustainable water purification remedies for future generations.

2. Materials and Methodology

2.1. Materials

Cupric oxide (CuO), Zinc nitrate hexa-hydrate (Zn $(NO_3)_2$.6 H_2O), methylene blue (MB), rhodamine dyes (Rh), and all other solvents with high purity 99 % (research grade) were purchased from Sigma Aldrich in Bangalore, India. The fresh coffee leaves were received from the Araku Coffee Garden, Visakhapatnam, Andhra Pradesh, India.

2.2. Fabrication process OF Cu-Zn-BMNPs

Fresh coffee leaves were thoroughly rinsed with deionized (DI) water to remove dust particles, and the surface moisture was naturally air-dried under sunlight. The dried leaves grounded into a fine powder. Phenolics such as chlorogenic acid, which have been identified in coffee leaves [54,55, 56], are known to reduce metal precursors [5]. Additionally, the presence of flavonoids like catechins contributes to nanoparticle stabilization through robust antioxidant activities [57]. A total of 2g of this powdered material was added with 75 mL of DI water in a 100 mL beaker and heated on a hot plate at 85 °C for 30 min with continuous stirring at 500 rpm. The resulting coffee leaf extract was subsequently filtered using a 125 mm Whatman filter paper. A precise method was followed to fabricate the Cu-Zn BMNPs catalyst. First, 50 mL of coffee leaf extract were gradually added drop by drop using a time controlled burette into a 200 mL beaker having a 20 % (w/v) solution of CuO and 80 % $Zn(NO_3)_2$. We tried different ratio of copper to zinc in the Cu-Zn BMNPs and 1:4 combination showed high photocatalytic activity. The nanoparticles mixture material was fabricated by placing it in hot plate at 90 °C temperature, with continuous stirring at 600 rpm for approximately about 30 min. The synthesis process continued until a distinct color change was observed in the nanoparticles mixture solution, indicating the formation of the nano-material catalyst. The mixture solution was centrifuged to get residue at 4000 rpm for 30–40 min, and the final nano-material was then dried in hot air oven at about 60 °C temperature to yield a fine nano-powder material. The Cu-Zn BMNPs demonstrate excellent long-term stability and reusability in repeated photocatalytic cycles for photo-catalytic activity and observed minimal loss in activity and structural integrity after multiple cycles. The illustration of the entire fabrication process and its mechanism of Cu-Zn BMNPs catalyst material is shown in Fig. 2.

The formation of Cu-Zn BMNPs occurs through the simultaneous reduction of Cu^{2+} and Zn^{2+} ions present in the reaction medium, utilizing coffee leaf extract as a green reducing and stabilizing agent. The plant extract contains biomolecules that facilitate the reduction of metal ions and stabilize the resulting BMNPs. The phytochemicals in the coffee leaf extract reduce Zn^{2+} and Cu^{2+} ions to their metallic states (Zn^0 and Cu^0).

$$Zn(NO_3)_2 + \text{Reducing Agent} \rightarrow Zn^0;\ Cu^{2+} + \text{Reducing Agent} \rightarrow Cu^0$$

In the synthesis of BMNPs involving Zn and Cu (ptimum doping), secondary metabolites such as phenolic compounds and flavonoids are crucial. These metabolites facilitate the reduction of metal ions Cu^{2+} and Zn^{2+} to their elemental forms (Cu^0 and Zn^0) while also stabilizing the resulting nanoparticles. The formation of BMNPs depends on the selection criteria for base material salts (Cu, Zn), and their bandgap values. Leaf extracts serve as both reducing and stabilizing agents in this process. Phenolic compounds contribute to the stabilization of the nanoparticles, while flavonoids play a key role in reducing the metal ions. Together, these compounds enhance the efficiency of nanoparticle synthesis through green chemistry methods.

As the reduced Zn^0 and Cu^0 nuclei form, they approach one another and coalesce into bimetallic structures through nucleation and growth processes. The phenolic and flavonoid compounds in coffee leaf extract play a vital role in preventing nanoparticle aggregation and stabilizing these nanoscale bimetallic structures. The intermixing of Zn^0 and Cu^0 atoms during nucleation creates unique configurations, such as core-shell or alloy-like structures. This results in the formation of Cu-Zn BMNPs with distinct structural and morphological properties, making them suitable for various applications.

2.3. Characterization OF Cu-Zn BMNPs

The Cu-Zn BMNPs nano-catalyst was characterized using UV–Vis absorption spectroscopy (UV-JASCO instrument), utilizing the Surface Plasmon Resonance (SPR) effect. This analysis enabled the detection of specific absorption peaks characteristic of the Cu-Zn BMNPs nano-catalyst. Fourier Transform Infrared Spectroscopy (FTIR-iS5) was performed within the spectral range of 400–4000 cm^{-1} to identify the biological or phytochemical functional groups involved in the eco-inspired synthesis of BMNPs. Furthermore, the surface morphology and their structural features of the Cu-Zn BMNPs catalyst was analyzed using Scanning Electron Microscopy (SEM) (ZEISS Merlin Compact instrument operating at 20 kV). The crystal structure, crystalline size, and phases of the Cu-Zn BMNPs nano-catalyst were analyzed using Powder X-Ray Diffraction (XRD) on a Bruker D8 Advance instrument. The XRD patterns, obtained with Cu-Kα radiation, offered detailed insights into the structural properties of the Cu-Zn BMNPs.

In summary, the comprehensive characterization of Cu-Zn BMNPs catalyst was achieved through various measurements. These characterization techniques collectively provided insights into their photocatalytic efficiency and essential material properties.

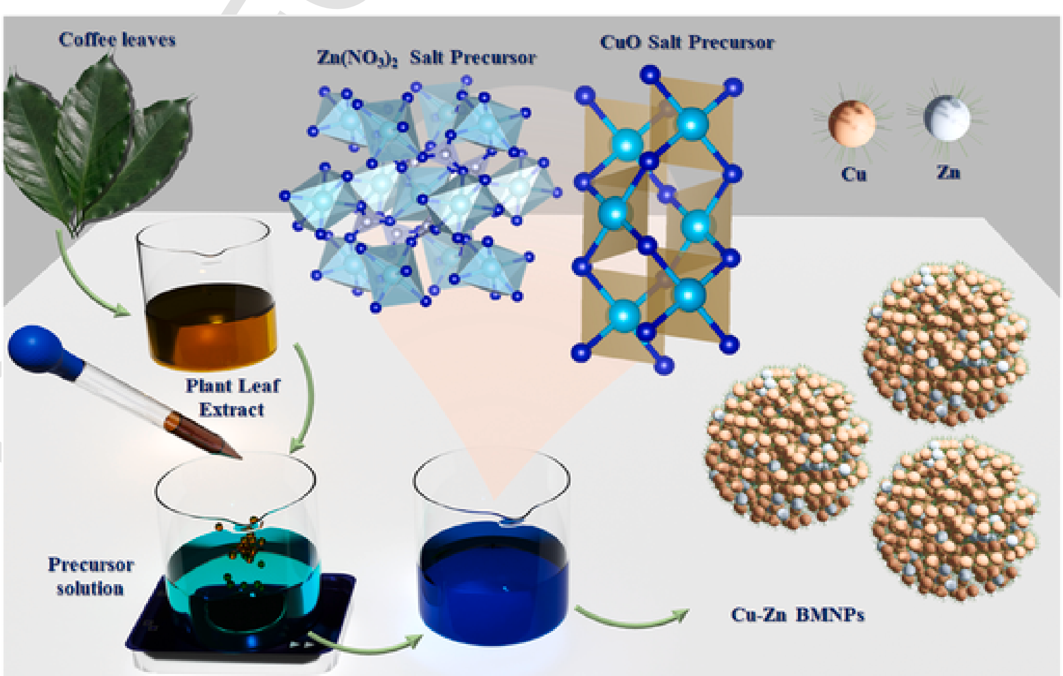

Fig. 2. Illustration of the fabrication process for the Cu-Zn BMNPs catalyst.

2.4. PHOTO-CATALYTIC activity – degree of dye degradation

The photocatalytic performance of the Cu-Zn BMNPs catalyst for the degradation of MB and Rh dyes was assessed under a 20W LED light source as a substitute for natural sunlight. The reaction was initiated by adding 3 mL of the Cu-Zn BMNPs nanocatalyst solution into a 50 ppm dye solution. The mixture was stirred in a dark environment for 20 min to allow the adsorption process to occur. Samples were taken at regular intervals, and their absorption peaks were examined under optimal conditions using UV–Vis spectroscopy. The UV–Vis absorption spectra revealed characteristic bands for MB at 668 nm and for Rh at 530 nm. Under visible light irradiation, the composite mixture solution was continuously stirred, and 3 mL aliquots of the suspension were collected at 30-min intervals over a total of 90 min to monitor changes in the absorption peaks of the both dyes. The percentage of dye degradation was determined using a formula cited in Ref. [46], utilizing data from the UV–Vis absorption spectra.

$$\text{Degradation } (\%) = \left(\frac{A_0 - A_t}{A_0}\right) \times 100$$

Where A_0 indicates the initial absorption at time $t = 0$, A_t indicates the absorption at a finite time t.

3. Results and discussion

3.1. Scanning electron microscopy (SEM)

The SEM images in Fig. 3 (a)-(d) illustrate the morphological characteristics of 20 % Cu-doped Zn BMNPs at various scales, alongside optimized Cu doping levels established in previous studies [19]. The Cu-doped Zn BMNPs exhibited a rod-like morphology, though the rod sizes were not uniformly distributed. The rod shaped morphology within the sample ranged widely in size, from 20 to 90 nm. The most of the Cu-Zn BMNPs nano catalyst exhibit a hexagonal shape but differ in sizes and rod shape morphology showed higher catalytic activity. Notably, the SEM micrographs of the Cu-Zn BMNPs also revealed smaller clusters of aggregated particles with different sizes. This clustering effect may result from diverse nucleation and growth dynamics of CuNPs and ZnNPs during the fabrication process.

Energy dispersive X-ray spectroscopy (EDS) was conducted to assess the copper content in Zn-based bimetallic nanoparticles (BMNPs), with the findings presented in Fig. 4. The chemical composition was found to be consistent across all samples. However, the detected levels of copper in the doped Zn nanoparticles (ZnNPs) were lower than the intended or nominal doping levels, likely due to the influence of nucleation and growth processes. The addition of copper atoms did not alter the structural uniformity of the ZnNPs. The Cu doping in Zn BMNPs were still consistent across samples and didn't impact the physical structure of the nanoparticles growth. This consistency and structural stability suggest that the doping process was controlled well enough to maintain the properties of the ZnNPs while introducing Cu atoms. This optimum Cu doping helped to improve the catalyst activity of Cu Zn BMNPs.

3.2. Fourier transform infrared spectroscopy

The FTIR spectrum of Cu-doped Zn BMNPs displayed characteristic bands at 3651, 2342, 1975.5, 1595.8, 1402, 1053, and 675 cm^{-1} indicated in Fig. 5. Biological functional groups from the coffee leaf extract acted as multifaceted agents during BMNP fabrication process, resulting in distinct alterations in the FTIR spectrum. These functional groups played an important role in improving stability of the Cu-Zn BMNPs catalyst [51]. The reduction of bi-metal precursors to form the BMNPs is likely attributed to the activity of functional groups present in compounds such as flavonoids and polyphenols. FTIR analysis of the recorded peaks facilitated the determining of functional groups present on the surface of the nano-catalyst material. The FTIR spectrum displayed a peak at 675 cm^{-1}, associated with the Cu-O stretching band, while the peak at 1595.8 cm^{-1} was linked to N-H stretching, ester carbonyl (C = O) groups, carboxylate ions (COO^-), and C-N/C-C stretching, suggesting the presence of proteins. Furthermore, a peak observed at 3307 cm^{-1} corresponded to phenolic compounds (OH stretching) derived from the leaf extract, which played a vital role in the eco-inspired synthesis and formation of the Cu-Zn BMNPs nano-catalyst.

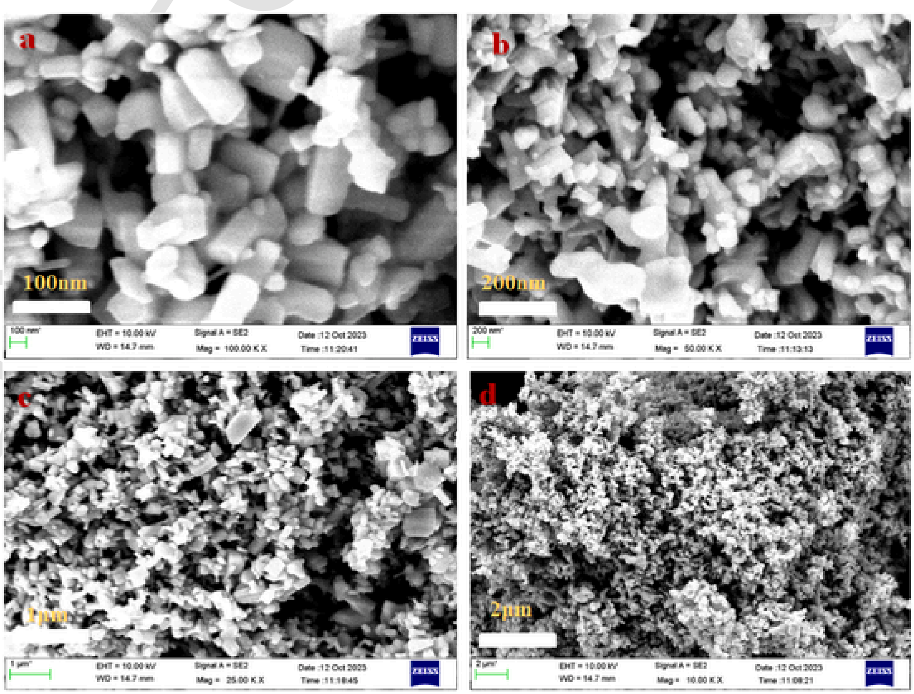

Fig. 3. SEM micrographs of coffee extract synthesized Cu doped Zn-BMNPs.

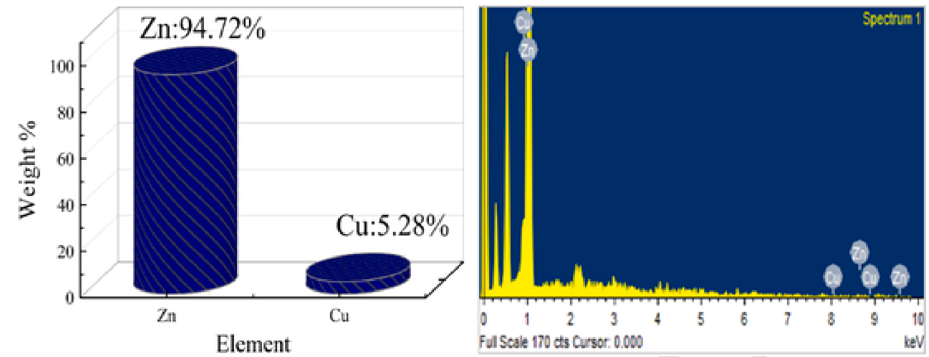

Fig. 4. SEM-EDS analysis of coffee extract synthesized Cu doped Zn-BMNPs.

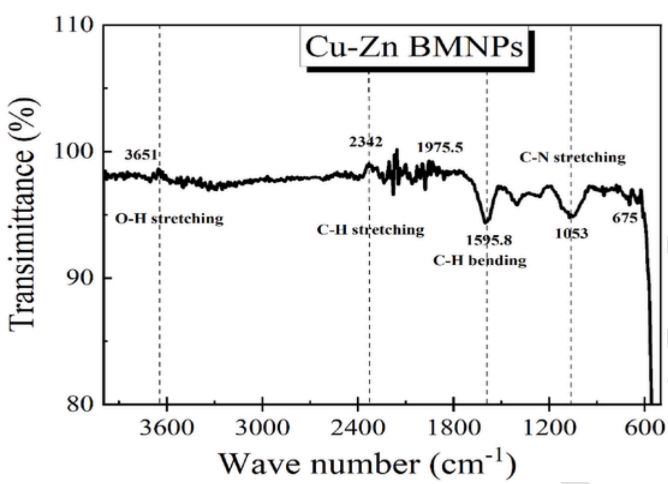

Fig. 5. FTIR spectrum of coffee leaf extract bio-synthesized Cu doped Zn-BMNPs.

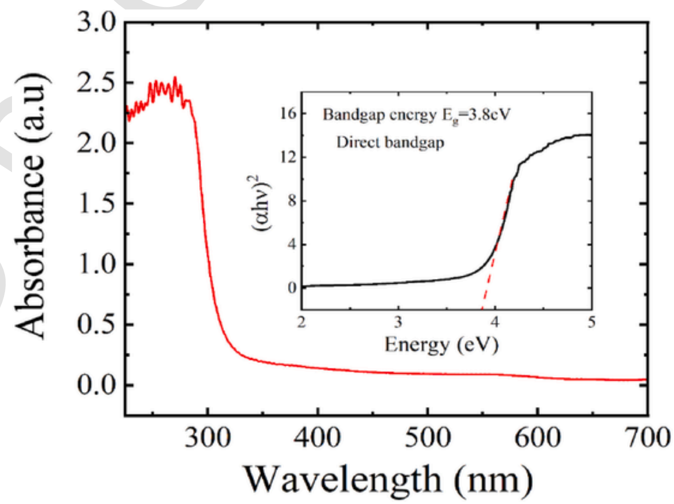

Fig. 6. UV–Vis absorption spectroscopy of coffee leaf extract synthesized Cu-Zn-BMNPs.

3.3. UV–VIS spectroscopy

The degree of absorption of eco-inspired synthesized Cu-doped Zn BMNPs were traced out using UV–Vis absorption spectroscopy. This study focused on examining the absorption peaks of nanocatalyst based on SPR using UV–Vis absorption spectroscopy. The Cu-doped Zn BM-NPs exhibited absorption peaks within the wavelength range of 250–470 nm, with the maximum peaks presented in Fig. 6. The bandgap energy was calculated to be 3.8 eV using the direct bandgap method through UV Tauc plot analysis ($(\alpha h\nu)^n$ vs $h\nu$). The absence of extra peaks in the UV–Vis analysis confirmed the lack of nanoparticle agglomeration in the Cu-Zn BMNPs.

3.4. X-RAY diffraction (XRD)

Fig. 7 presents the XRD spectrum of Cu-Zn BMNPs, showing distinct intensity peaks at 2θ values of 31.5°, 33.9°, 35.9°, 47.2°, 56.2°, 62.6°, and 67.6°. The XRD spectrum was analyzed using the X'pert High Score Plus software to determine the 2θ values for ZnNPs, CuNPs, and Cu-Zn BMNPs samples. For ZnNPs, the crystallographic planes identified were (100), (002), (101), (102), (110), (103), and (112), aligning with the hexagonal phase as per the JCPDS data sheet 04-005-5076 [52]. Similarly, for CuNPs, peaks at 2θ values of 32.4°, 35.2°, 48.4°, and 66.1° were attributed to the planes (111), (002), (202), and (311), consistent with the monoclinic phase and referenced in the JCPDS data sheet 01-086-8837 [53]. The average crystalline size of Cu-Zn BMNPs catalyst

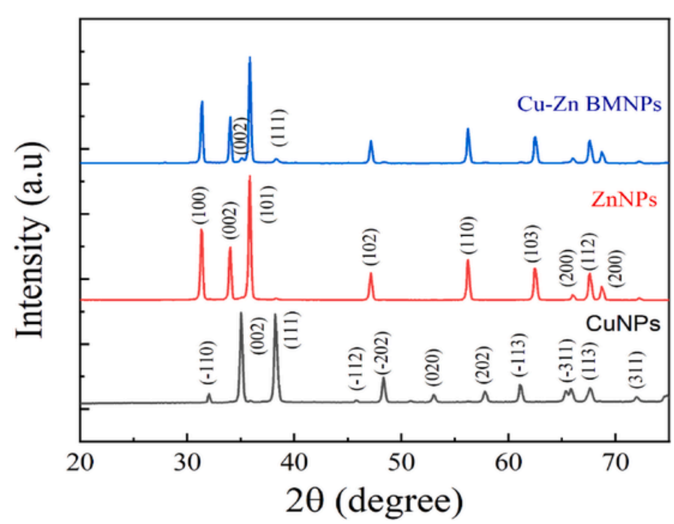

Fig. 7. XRD spectrum of coffee extract based Cu doped Zn BMNPs.

synthesized using coffee leaf extract was determined using the Debye-Scherrer equation, yielding a crystalline size range from 10 to 36 nm. The detailed crystalline size calculations for CuNPs, ZnNPs, and Cu-ZnNPs are mentioned in Table 1. ZnNPs exhibited slightly higher peak intensities compared to both CuNPs and Cu-Zn BMNPs materials. Additionally, Cu-Zn BMNPs catalyst displayed improved nucleation growth and crystallinity. The reduction in peak intensity and crystallinity for Cu-Zn BMNPs could be related to the surface coating effect of ZnNPs [53,54]. The XRD patterns of Cu-Zn BMNPs revealed crystalline structures characteristic of nanocatalyst, with dominant peaks corresponding to Zn and only a few peaks attributed to Cu. The minimal presence of Cu peaks in the Cu-Zn BMNPs suggests that Cu atoms may have been incorporated into the ZnNP lattice. These observations provide strong evidence for the presence of a crystalline phases within the Cu-Zn BMNPs. Additionally, primary reflections corresponding to Cu (111) plane provide further supports the crystalline nature of Cu-Zn BMNPs. Fig. 7 shows an XRD peak shift for Cu-Zn BMNPs at the (110) plane when compared to pure ZnNPs. This slight shift in the peak position upon Cu doping is likely due to the small difference in the ionic radii of both Cu^{2+} (0.73 Å) and Zn^{2+} (0.74 Å), as well as variations in the lattice constants. An increase in the lattice parameters was observed for Cu-doped Zn BMNPs catalyst when compared to the pristine ZnNPs sample. The crystal lattice constants were determined by using the Braggs equation.

$$a = \lambda \left(\frac{\sqrt{h^2 + k^2 + l^2}}{2 \sin \theta} \right) A^0.$$

The crystallite size of the Cu-Zn BMNPs catalyst was determined using the Debye-Scherrer equation: $D = 0.9\lambda/\beta\cos\theta$, where λ indicates wavelength of the X-rays, β indicates the full width at half maximum (FWHM) of the diffraction peak, and 2θ is the Bragg angle. The precise mechanism underlying the synthesis of Cu-Zn BMNPs catalyst using plant leaf extract is not fully understood. However, it is suggested that the color change observed within 30–40 min of the reaction may be attributed to oxidation, which perform a significant role in facilitating the formation of BMNPs nano-catalyst. Additionally, electrostatic interactions are believed to play a crucial role in stabilizing metal oxide ions, facilitating the nucleation of stable nanoparticles, and preventing the aggregation of Cu-Zn BMNPs clusters. Although the underlying mechanisms of metal nano particles bio-synthesis remain under study, the application of plant leaf extracts in the production of Cu-Zn BMNPs emphasizes the potential of biogenic green synthesis methods. This approach is particularly promising due to its environmental sustainability, non-toxicity, and cost-effectiveness, offering a valuable pathway for researchers seeking to develop eco-inspired synthesis and sustainable techniques for metal nanoparticles fabrication.

Table 1
The diffraction peak angles and crystalline sizes of CuNPs, ZnNPs and Cu-Zn BMNPs.

S.NO	2θ (CuNPs)	Crystalline size (nm)	2θ (ZnNPs)	Crystalline size(nm)	2θ(Cu-Zn BMNPs)	Crystalline size (nm)
1	35	21.9	31.34	39.3	31.35	43
2	38.2	44.1	34	44	34	44
3	48.3	44.5	35.8	44.2	35.8	30
4	50.87	46.1	47.15	31.2	47	45
5	61.13	46.5	56.23	32.4	56	32
6	67.7	45.5	62.5	49.2	62.5	33.4
7	74.7	34.4	67.6	34.4	76	28

3.5. Photo-catalytic activity of Cu-Zn-BMNPs nano-catalyst

Fig. 8(a and b) illustrates the photocatalytic performance of the Cu-Zn-BMNPs catalyst in degrading MB and Rh dyes at their optimal concentration of 50 ppm. The degradation efficiency is influenced by several factors, including exposure duration, light source intensity, dye concentration, and catalyst dosage. In this investigation, a 20W LED bulb was employed as the light source for testing degradation. The exceptional catalytic efficiency of the Cu-Zn-BMNPs is primarily due to it has high energy gap and surface-to-volume ratio, which improve its degradation efficacy. Liquid samples of the catalyst were collected at regular intervals during light exposure and analyzed using UV–Vis spectroscopy to track changes in absorbance. The results indicated a consistent decrease in absorption intensity with prolonged exposure to light. Fig. 8 (a-b) illustrates the degradation process, indicating the absorbance patterns of MB and Rh dyes with introduction of the Cu-Ag-BMNPs catalyst. These results emphasize that the incorporation of CuO into the Zn BMNPs structure, along with surface modification, significantly improve photocatalytic performance.

The Cu-Zn BMNPs nanocatalyst exhibits remarkable efficiency in degrading MB and Rh dyes, as evidenced by a significant reduction in absorption intensity from 2.5 to 0.19 for MB dye and from 3.3 to 0.15 for Rh dye using a 3 mL concentration of the catalyst (Fig. 9). Interestingly, Rh dye shows higher absorption compared to MB dye under identical conditions. The optimal concentration of the Cu-Zn BMNPs catalyst offers an increased surface area, facilitating efficient interactions and the adsorption of toxic dye molecules. The photocatalytic mechanism relies on the absorption of light, generating electron-hole pairs that drive the breakdown of dye toxic molecules.

The Cu-Zn BMNPs catalyst exhibited an optical energy band gap of around 3.8 eV, as calculated from UV data. This value was further confirmed through the Tauc plot approach and analysis of the absorption spectrum, shown in Fig. 6. This research highlights the potential environmental applications of the BMNPs nano-catalyst within the advanced engineering industrial sector. The degradation of MB and Rh dyes is mainly driven by the activity of oxygen and hydroxyl radicals, which are crucial in breaking down toxic components of these two dyes.

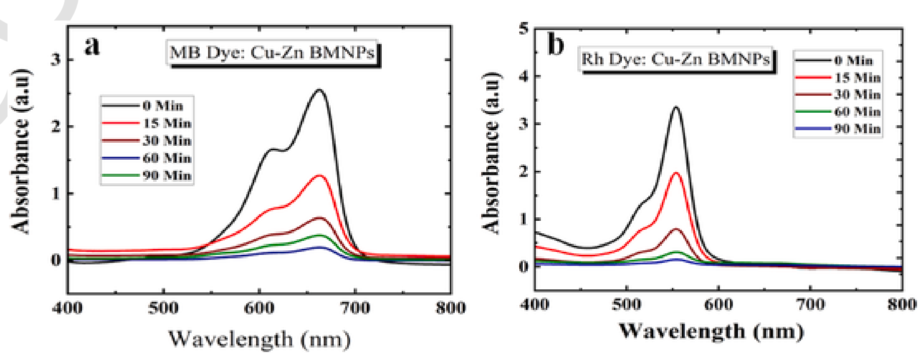

Fig. 8. Photocatalytic performance of coffee extract synthesized Cu-Zn-BMNPs catalyst (a) MB dye (b) Rh dye.

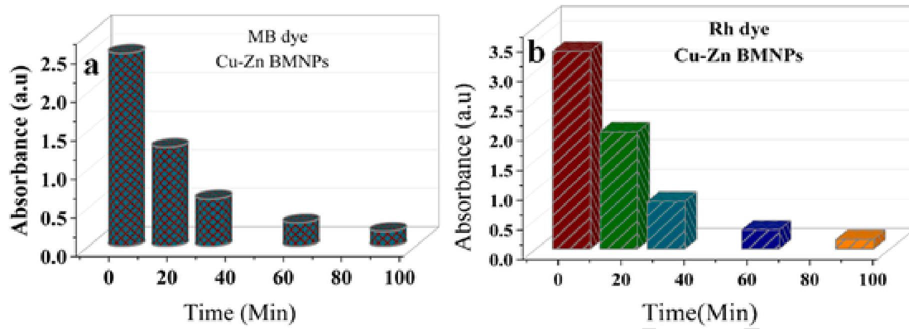

Fig. 9. Absorption of MB (a) & Rh (b) dyes with respect to time (Minutes) at 3 mL Cu-Zn BMNPs catalyst concentration.

As light exposure time increases, the dyes exhibit a noticeable change color, gradually transitioning to lighter shades or becoming entirely colorless. The degradation efficiencies for Rh and MB dyes at a 50 ppm concentration were determined to be approximately 95.2 % and 92.4 %, respectively, using 3 mL of the Cu-Zn BMNPs catalyst concentration, as shown in Fig. 10. The degradation efficiency was measured over a 90-min exposure to a 20W LED light source, using 3 mL of the Cu-Zn BMNPs photocatalyst. Notably, Rh dye exhibited a higher degradation rate compared to MB dye under the same catalyst concentration, indicating active interactions between the catalyst and Rh dye, leading to more pronounced degradation during the reduction process. This finding underscores the intricate dynamics of photocatalytic dye degradation and offers valuable insights for future research in this field.

3.5.1. *KINETIC STUDIES of BIOGENIC Cu-Zn-BMNPs CATALYST*

The first-order kinetic theory equation was employed to evaluate the photocatalytic response and dye degradation kinetic mechanism of MB and Rh dyes using the BMNPs value added material. The suitable model is mathematically expressed as $\ln\left(\frac{A_0}{A_t}\right) = kt$

In this first-order kinetic model equation, A_0 represents the initial dye absorbance intensity at $t = 0$, A_t denotes the absorbance intensity of the dye at a later time t, and k is the rate constant. In our study, we extensively examined the kinetics of dye photo-degradation catalyzed by the Cu-Zn BMNPs nano-catalyst, with the findings clearly presented through a detailed analysis shown in Fig. 11 $\ln\left(\frac{A_0}{A_t}\right)$ versus light exposure time for (a) MB dye and (b) Rh dye at optimum 3 mL BMNPs catalyst concentration. The first order rate constant (k) for both dyes indicate slope of straight line between $\ln\left(\frac{A_0}{A_t}\right)$ and irradiation time. A detailed analysis of the kinetic photo-degradation of dyes using the Cu-Zn BMNPs catalyst was conducted, with the results shown in Fig. 11. The degradation rate was evaluated using the first-order kinetic model, and the rate constant was determined from the slope of the fitted line, which is essential for understanding the biosynthesis process of the Cu-

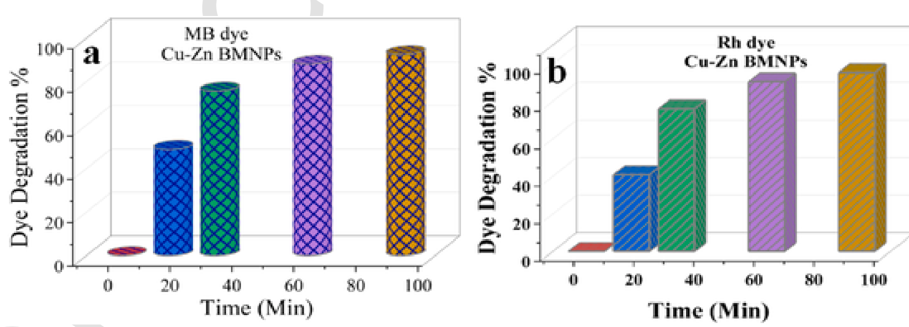

Fig. 10. Photocatalytic performance of Cu-Zn-BMNPs nano-catalyst at 50 ppm both MB (a) and Rh (b) dyes.

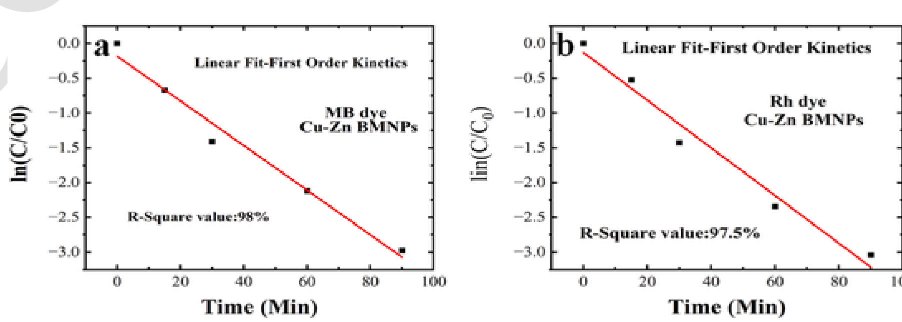

Fig. 11. Kinetics analysis of dye degradation for both MB and Rh dyes.

Zn BMNPs catalyst. Under visible light exposure, biomolecules and phytochemicals from the coffee leaf extract facilitated electron transfer from the valence band to the conduction band in the Cu-Zn BMNPs material. This process led to the generation of superoxide and hydroxyl radicals, enhancing the photocatalytic activity of the Cu-Zn BMNPs catalyst. These findings provide valuable insights into the complex mechanisms underlying the photocatalytic activity of the Cu-Zn BMNPs nanocatalyst, emphasizing their potential for environmental and water purification industrial applications [51,52].

3.5.2. Possible mechanism OF Cu-Zn-BMNPs nano-catalyst

The challenges involved in the detoxification of toxic MB and Rh dye molecules under light exposure were explored through the photocatalytic dye degradation process. Fig. 12 illustrates the proposed fundamental mechanism for the photocatalytic breakdown of MB and Rh dyes. The Cu-doped Zn BMNPs catalyst, with its narrow energy band gap, acts as a promising nano-catalyst by facilitating the generation of rich electron-hole pairs and minimizing their recombination process. This efficiency can be attributed to the small amount of energy required for electrons to transition from higher occupied to lower unoccupied energy states. Upon light exposure, the Cu-Ag BMNPs catalyst absorbs energy corresponding to its band gap, initiating the photocatalytic process.

The transition of electrons from a lower to an excited energy state involves several key elements, including the band gap, a hole in the valence band (h^+), a released electron, and an electron in the conduction band (e^-). Among these, the hole in the valence band plays a crucial role as an electron acceptor, extracting electrons from pollutant molecules and initiating the degradation of dyes. This process contributes to the formation of highly reactive species, with water molecules being converted into hydroxyl radicals (OH•), which are essential for breaking down organic toxic molecules. At the same time, oxygen molecules interact with electrons to generate superoxide radicals (O_2•$^-$). The reduction of pollutants occurs through these mechanisms, facilitating an efficient dye degradation process.

$$\text{Photcatalyst Cu} - \text{Zn BMNPs} + h\nu \rightarrow e^- + h^+$$
$$\text{Photcatalyst BMNPs } (\text{e}^-) + h\nu \rightarrow O_2^-$$
$$\text{Photcatalyst BMNPs } \left(\text{h}^+\right) + H_2O \rightarrow OH^-$$
$$O_2^- \, (or) \, OH^- + MB/Rd \; dyes \rightarrow \text{Degraded material}$$

Advanced oxidation process (AOP) is crucial step in understanding how reactive oxygen species (ROS), such as hydroxyl radicals (-OH) and superoxide radicals (-O_2^-), are generated during photocatalysis. The AOP involves generating radicals of hydroxyl through reactions involving water molecules and photogenerated holes (h^+). These free radicals are highly reactive and play a significant role in degrading organic pollutants or dyes. ROS contribute to breaking down dye molecules into less harmful byproducts, enhancing overall degradation efficiency. The dye concentration, catalyst concentration & intensity of light, reaction kinetics, these free radicals play important role oral improving dye degradation efficiency. This mechanism provides important insights into the complex pathway through which all dye contaminates in water are effectively removed. The optimum Cu doping of Cu-Zn BMNPs helps to enhance catalytic activity due to faster releasing charge carriers and lead to improve the dye degradation efficiency.

Our findings confirm that oxide and hydroxyl radicals are the primary reactive species involved in the photocatalytic degradation of water-soluble dyes. This process enhances long term effectiveness of the photocatalytic process and highlights the potential of the Cu-Zn-BMNPs catalyst for sustainable environmental remediation in industrial applications.

3.5.3. Factors affecting-photocatalytic degradation OF Cu-Zn-BMNPs catalyst

Achieving optimal photocatalytic performance involves considering several factors, such as dye concentration, photo-catalyst concentration, secondary metabolites, selection two metal salts based on optical band gap, AOP, ROS, catalyst structure, morphology, type of irradiation, exposure time, and the light source. At higher dye concentrations, an inhibitory effect is observed, primarily due to a reduction in interactions with the active sites of the nano-catalyst. As the dye concentration increases, the light absorption capacity of the dye molecules decreases, which subsequently limits the migration of electrons to the photo-

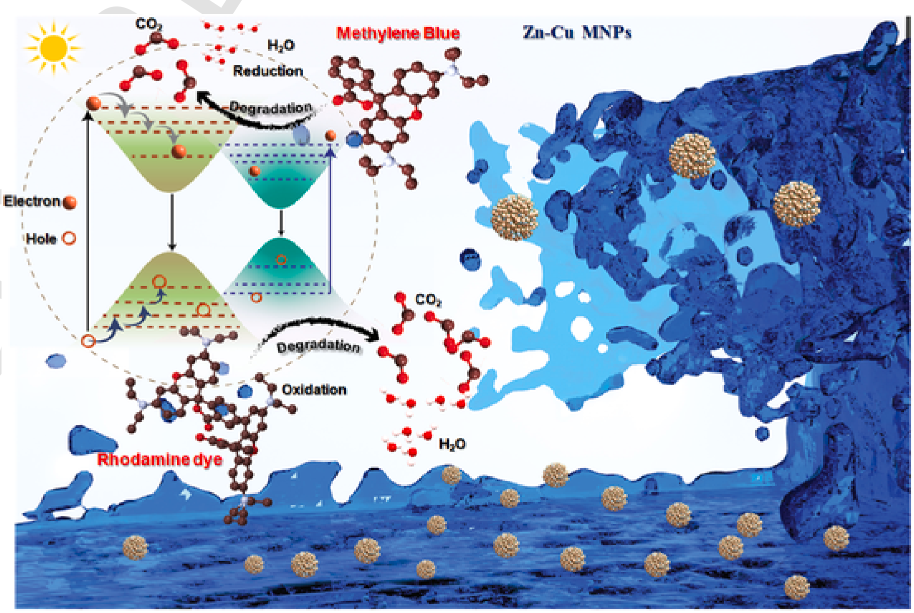

Fig. 12. Schematic of photo-catalytic performance for coffee leaf extract Cu-Zn BMNPs nano-catalyst.

catalyst material. Consequently, fewer hydroxyl radicals are produced, leading to a decrease in the efficiency of the dye degradation process. Our findings demonstrate that a 50 mg/L (50 ppm) concentration of both MB and Rh dye solutions yields the best results for effective degradation. As the concentration of the photo-catalyst increases, or reaches its optimal level, the number of active sites also increases, leading to a higher production of e^{-}-h pairs. The continuous generation of ROS through optimized AOPs contributes to sustainable catalytic activity over time, making these processes suitable for long-term applications in wastewater treatment. This mechanism helps to increase the production of hydroxyl radicals, which are critical for the efficient dye degradation of organic pollutants. The morphological properties, size, and shape of the Cu-Zn-BMNPs nanocatalyst stand a significant role in enhancing the effectiveness of dye degradation. Notably, the degradation of Rh dye exhibits a more pronounced activity compared to MB dye. Cu-doped Zn BMNPs catalysts with smaller particle sizes exhibit improved effectiveness due to their ability to provide more active sites for dye adsorption. In our study, using a 3 mL concentration of the Cu-Zn BMNPs catalyst with a 50 ppm dye concentration resulted in significant degradation rates: 95.2 % for Rh dye and 92.4 % for MB dye within 90 min. Notably, the Cu-Zn BMNPs nanocatalyst was synthesized through a simple, eco-inspired biosynthesis method using coffee leaf extract. These findings highlight the considerable potential of our Cu-doped Zn BMNPs catalyst as a photo catalyst, making it suitable for various sustainable water purification applications. The catalytic activity of the Cu-Zn BMNPs could potentially be further enhanced by doping with carbon nanotubes (CNTs). CNTs are known for their exceptional electrical conductivity, high surface area, and strong adsorption capacity, which can improve charge separation, reduce recombination of e^{-}-h pairs, and provide additional reactive sites.

4. Conclusion

This work focuses on the eco-friendly synthesis of a cost-effective nanocatalyst, achieved by doping Cu with Zn BMNPs using coffee leaf extracts. Comprehensive characterization techniques confirmed the successful development of the Cu Zn BMNPs. Optical studies indicated that the synthesized material exhibits activity under UV–Vis light, with the direct optical bandgap value determined to be 3.8 eV. The biosynthesized nano-catalyst demonstrated remarkable efficiency in the photocatalytic degradation of MB and Rh dyes, achieving degradation rates of 95.2 % for MB and 92.4 % for Rh under optimal conditions. Kinetic analysis indicated that the degradation of both dyes showed pseudo-first-order reaction kinetics. Hydroxyl radicals were identified as the key reactive oxidant species driving the degradation process in the presence of a 20W LED light source. Our future research will focus on developing film-based, foldable polymer nanocomposites and evaluating their photocatalytic performance with doping CNTs for different dyes. The eco-friendly bio-synthesis method highlights a sustainable approach, reducing the use of harmful chemicals. These combined efforts aim to enable scalable industrial production, contributing to advancements in environmental applications and human health. In conclusion, this study demonstrates that the bio-synthesized material has significant potential for photocatalytitreatment of wastewater contaminated with diverse pollutants.

Uncited References

[47]; [49]; [50]; [56].

CRediT authorship contribution statement

Naveen Kumar Dabbeta: Investigation, Formal analysis, Data curation. **Kante Mamtha:** Data curation. **Koda Ramya:** Data curation. **Devarala Abhilash:** Data curation. **Pranay Bhaskar Kalakonda:** Formal analysis, Data curation. **Sarvani Jowhar Khanam:** Data curation. **Ramu Naidu Savu:** Data curation. **Murali Banovath:** Data curation. **S. Laxmi Srinivass Rao:** Data curation. **B. Vijaya Nirmala:** Data curation. **Imran Hasan:** Validation, Methodology. **Parvathalu Kalakonda:** Visualization, Supervision, Project administration, Conceptualization.

Data availability

Data is provided with the request of readers.

Ethical approval

The institute's Research and Development Committee has reviewed and granted consent for the publication of this work.

Funding

No funding was received for this project.

Declaration of interest

I hereby declare my intent to submit the work, titled "**Eco-Inspired Cu-Zn Bimetallic Nanocomposites for Enhanced Water Purification Technologies**," to the **Materials Chemistry and Physics: Sustainability and Energy**.

The content presented is an original work, and I confirm that the responses provided, including the abstract, paragraph, and graphical abstract, are accurate representations of the information derived from the dataset provided. I understand and acknowledge that the decision to accept this submission with the editorial board of the **Materials Chemistry and Physics: Sustainability and Energy**.

I agree to comply with reviewer suggestions for improvement of this high standard manuscript. Additionally, I affirm that this work has not been published elsewhere, and I commit to informing the editorial board promptly if there are any changes in this regard. This resubmission adheres to the ethical standards and guidelines of academic research, and I take responsibility for the authenticity and integrity of the content presented.

Acknowledgement

1.The authors extend their thanks to Smart Nano material Research Laboratory (SNRL), Dept. of Physics, Government City College (Autonomous); NAAC A++ CGA:3.67 for supporting basic facilities and characterization of materials.

2.The authors extend their thanks to researchers supporting project (Ref: RSPD2023R670), King Saud University, Riyadh, KSA.

Data availability

Data will be made available on request.

References

[1] T. Rajaram, A. Das, Water pollution by industrial effluents in India: discharge scenarios and case for participatory ecosystem-specific local regulation, Futures 40 (1) (2008) 56–69.
[2] M.F. Hanafi, N. Sapawe, A review on the water problem associated with organic pollutants derived from phenol, methyl orange, and remazol brilliant blue dyes, Mater. Today Proc. 31 (2020) 141–150.
[3] T. Islam, M. Repon, T. Islam, et al., Impact of textile dyes on health and ecosystem: a review of structure, causes, and potential solutions, Environ. Sci. Pollut. Res. 30 (2023) 9207–9242.
[4] K.G. Pavithra, V. Jaikumar, Removal of colorants from wastewater: a review on sources and treatment strategies, J. Ind. Eng. Chem. 75 (2019) 1–19.
[5] M. Ismail, K. Akhtar, M. Khan, T. Kamal, M.A. Khan, A. M Asiri, J. Seo, S.B. Khan, Pollution, toxicity, and carcinogenicity of organic dyes and their catalytic bioremediation, Curr. Pharm. Des. 25 (2019) 36453–36663.

[6] I. Khan, K. Saeed, I. Zekker, B. Zhang, A.H. Hendi, A. Ahmad, et al., Review on methylene blue: its properties, uses, toxicity, and photodegradation, Water 14 (2) (2022) 242.
[7] R.H. Waghchaure, V.A. Adole, B.S. Jagdale, Photocatalytic degradation of methylene blue, rhodamine B, methyl orange and Eriochrome black T dyes by modified ZnO nanocatalysts: a concise review, Inorg. Chem. Commun. 143 (2022) 109764.
[8] M. Ismail, K. Akhtar, M.I. Khan, T. Kamal, M.A. Khan, A. M Asiri, et al., Pollution, toxicity, and carcinogenicity of organic dyes and their catalytic bio-remediation, Curr. Pharm. Des. 25 (34) (2019) 3645–3663.
[9] U. Shanker, M. Rani, V. Jassal, Degradation of hazardous organic dyes in water by nanomaterials, Environ. Chem. Lett. 15 (2017) 623–642.
[10] M.L. Sall, A.K.D. Diaw, D. Gningue-Sall, S. Efremova Aaron, J.J. Aaron, Toxic heavy metals: impact on the environment and human health, and treatment with conducting organic polymers, a review, Environ. Sci. Pollut. Res. 27 (2020) 29927–29942.
[11] M. Ebrahimi, N. Khalili, S. Razi, M. Keshavarz-Fathi, N. Khalili, N. Rezaei, Effects of lead and cadmium on the immune system and cancer progression, J. Environ. Health Sci. Eng. 18 (2020) 335–343.
[12] M. Shabir, M. Yasin, M. Hussain, I. Shafiq, P. Akhter, A.S. Nizami, et al., A review on recent advances in the treatment of dye-polluted wastewater, J. Ind. Eng. Chem. 112 (2022) 1–19.
[13] A. Rafiq, M. Ikram, S. Ali, F. Niaz, M. Khan, Q. Khan, M. Maqbool, Photocatalytic degradation of dyes using semiconductor photocatalysts to clean industrial water pollution, J. Ind. Eng. Chem. 97 (2021) 111–128.
[14] H. Kumari, Sonia, R. Suman, R. Ranga, S. Chahal, S. Devi, et al., A review on photocatalysis used for wastewater treatment: dye degradation, Water Air Soil Pollut. 234 (6) (2023) 349.
[15] C.V. Reddy, K.R. Reddy, V.A. Harish, J. Shim, M. Shankar, N.P. Shetti, T.M. Aminabhavi, Metal-organic frameworks (MOFs)-based efficient heterogeneous photocatalysts: synthesis, properties and its applications in photocatalytic hydrogen generation, CO2 reduction and photodegradation of organic dyes, Int. J. Hydrogen Energy 45 (2020) 7656–7679.
[16] A. Bassi, P. Kalakonda, I. Hasan, Synthesis of Chitosan-Agar immobilized NiO-MgO bionanocomposites and their photocatalytic application towards toxic azo dye, Inorg. Chem. Commun. (2024) 113499.
[17] I. Hasan, A. Bassi, P. Kalakonda, K. Kanungo, ZnO-doped kaolin nanoclay immobilized agar biopolymer for 2, 4-dinitrophenol photocatalytic degradation, Asia Pac. J. Chem. Eng. (2024) e3144.
[18] P. Kalakonda, M. Thodeti, C. Ganneboina, K. Ankathi, S. Kathri, K. Begari, et al., Eco-friendly fabrication of silver nanoparticles for sustainable water purification and antibacterial synergy, Plasmonics (2024) 1–13.
[19] P. Kalakonda, A. Bashitangu, P. Mandal, S.J. Khanam, M. Banovath, I. Hasan, B.B. Podila, Sustainable solutions for clean water: green synthesized Cu-Ag-Bimetallic nanoparticles-based nano catalyst, Mater. Sci. Eng. B 301 (2024) 117147.
[20] A. Philip, A.R. Kumar, The performance enhancement of surface plasmon resonance optical sensors using nanomaterials: a review, Coord. Chem. Rev. 458 (2022) 214424.
[21] M.A. Shenashen, S.A. El-Safty, E.A. Elshehy, Synthesis, morphological control, and properties of silver nanoparticles in potential applications, Part. Part. Syst. Char. 31 (3) (2014) 293–316.
[22] P. Kalakonda, P.B. Kalakonda, S. Banne, Studies of electrical, thermal, and mechanical properties of single-walled carbon nanotube and polyaniline nanoporous nanocomposites, Nanomater. Nanotechnol. 11 (2021) 18479804211001140.
[23] J. Li, J.Z. Zhang, Optical properties and applications of hybrid semiconductor nanomaterials, Coord. Chem. Rev. 253 (23–24) (2009) 3015–3041.
[24] U. Qumar, J.Z. Hassan, R.A. Bhatti, A. Raza, G. Nazir, W. Nabgan, M. Ikram, Photocatalysis vs adsorption by metal oxide nanoparticles, J. Mater. Sci. Technol. 131 (2022) 122–166.
[25] İ. Polat, S. Yılmaz, İ. Altın, E. Bacaksız, M. Sökmen, The influence of Cu-doping on structural, optical and photocatalytic properties of ZnO nanorods, Mater. Chem. Phys. 148 (3) (2014) 528–532.
[26] H. Kumari, Sonia, R. Suman, R. Ranga, S. Chahal, S. Devi, et al., A review on photocatalysis used for wastewater treatment: dye degradation, Water Air Soil Pollut. 234 (6) (2023) 349.
[27] K. Parvathalu, K. Rajitha, B. Chandrashekar, K. Sathvik, K. Pranay Bhasker, B. Sreenivas, et al., Biomimetic synthesis of copper nanoparticles using Tinospora cordifolia plant leaf extract for photocatalytic activity applications, Plasmonics 19 (2) (2024) 825–834.
[28] P. Kalakonda, M. Thodeti, C. Ganneboina, K. Ankathi, S. Kathri, K. Begari, et al., Eco-friendly fabrication of silver nanoparticles for sustainable water purification and antibacterial synergy, Plasmonics (2024) 1–13.
[29] Y. Cui, S. Hong, W. Jiang, X. Li, X. Zhou, X. He, et al., Engineering mesoporous bioactive glasses for emerging stimuli-responsive drug delivery, Biomater. Sci. 12 (7) (2024) 2008–2019.
[30] J. Daimari, A.K. Deka, Anticancer, antimicrobial and antioxidant activity of CuO–ZnO bimetallic nanoparticles: green synthesised from *Eryngium foetidum* leaf extract, Sci. Rep. 14 (1) (2024) 19506.
[31] S. Dubey, T. Virmani, S.K. Yadav, A. Sharma, G. Kumar, A. Alhalmi, Breaking barriers in eco-friendly synthesis of plant-mediated metal/metal oxide/bimetallic nanoparticles: antibacterial, anticancer, mechanism elucidation, and versatile utilizations, J. Nanomater. 2024 (1) (2024) 9914079.
[32] K. Parvathalu, S. Chinmayee, B. Preethi, A. Swetha, G. Maruthi, M. Pritam, P.B. Bhaskar, Green synthesis of silver nanoparticles using *Argyreia nervosa* leaf extract and their antimicrobial activity, Plasmonics 18 (3) (2023) 1075–1081.
[33] P. Kalakonda, S. Banne, Synthesis and optical properties of highly stabilized peptide-coated silver nanoparticles, Plasmonics 13 (2018) 1265–1269.
[34] P. Kalakonda, B. Sreenivas, Synthesis and optical properties of highly stabilized peptide-coated gold nanoparticles, Plasmonics 12 (2017) 1221–1225.
[35] S. Dubey, T. Virmani, S.K. Yadav, A. Sharma, G. Kumar, A. Alhalmi, Breaking barriers in eco-friendly synthesis of plant-mediated metal/metal oxide/bimetallic nanoparticles: antibacterial, anticancer, mechanism elucidation, and versatile utilizations, J. Nanomater. 2024 (1) (2024) 9914079.
[36] P. Kalakonda, Synthesis of silver nanowires for highly conductive and transparent films, Nanomater. Nanotechnol. 6 (2016) 1847980416663672.
[37] P. Kalakonda, P.B. Kalakonda, S. Banne, Studies of electrical, thermal, and mechanical properties of single-walled carbon nanotube and polyaniline nanoporous nanocomposites, Nanomater. Nanotechnol. 11 (2021) 18479804211001140.
[38] E. Yohannis, T.A. Teka, J.A. Adebo, M.M. Urugo, A. Hossain, T. Astatkie, Phytochemical constituents, ethnomedicinal uses, and applications of coffee (*Coffea arabica*) leaves in functional beverages, J. Food Compos. Anal. (2024) 106570.
[39] R. Acidri, Y. Sawai, Y. Sugimoto, T. Handa, D. Sasagawa, T. Masunaga, E. Nishihara, Phytochemical profile and antioxidant capacity of coffee plant organs compared to green and roasted coffee beans, Antioxidants 9 (2) (2020) 93.
[40] F. de Abreu Pinheiro, L.F. Elias, M. de Jesus Filho, M.U. Modolo, J.D.C.G. Rocha, M.F. Lemos, W.S. Cardoso, Arabica and Conilon coffee flowers: bioactive compounds and antioxidant capacity under different processes, Food Chem. 336 (2021) 127701.
[41] O.O. Ogochukwu, M.B. Fabiyi, O.S. Aworunse, O.A. Oyewole, P.O. Isibor, Nanoparticle properties and characterization, in: Environmental Nanotoxicology: Combatting the Minute Contaminants, Springer Nature Switzerland, Cham, 2024, pp. 23–40.
[42] A.J. Shnoudeh, I. Hamad, R.W. Abdo, L. Qadumii, A.Y. Jaber, H.S. Surchi, S.Z. Alkelany, Synthesis, characterization, and applications of metal nanoparticles, in: Biomaterials and Bionanotechnology, Academic Press, 2019, pp. 527–612.
[43] V. Molahalli, A. Sharma, K. Bijapur, G. Soman, A. Shetty, B. Sirichandana, G. Hegde, Properties, synthesis, and characterization of Cu-based nanomaterials, in: Copper-Based Nanomaterials in Organic Transformations, American Chemical Society, 2024, pp. 1–33.
[44] S.M. Naghib, M. Bakhshi, B. Ahmadi, A. Bakhshi, Gold nanoparticles based antibacterial and antiviral functional materials, in: Antibacterial and Antiviral Functional Materials, vol. 2, American Chemical Society, 2024, pp. 221–256.
[45] K. Ahmad, M.S. Khan, A. Iqbal, E. Potrich, L.S. Amaral, S. Rasheed, M. Ashfaq, Lead in drinking water: adsorption method and role of zeolitic imidazolate frameworks for its remediation: a review, J. Clean. Prod. 368 (2022) 133010.
[46] C. Nobile, P.D. Cozzoli, Synthetic approaches to colloidal nanocrystal heterostructures based on metal and metal-oxide materials, Nanomaterials 12 (10) (2022) 1729.
[47] I.V. Gürsel, T. Noël, Q. Wang, V. Hessel, Separation/recycling methods for homogeneous transition metal catalysts in continuous flow, Green Chem. 17 (4) (2015) 2012–2026.
[48] J.M. Thomas, R. Raja, The advantages and future potential of single-site heterogeneous catalysts, Top. Catal. 40 (2006) 3–17.
[49] P. Lakhani, D. Bhanderi, C.K. Modi, Nanocatalysis: recent progress, mechanistic insights, and diverse applications, J. Nanoparticle Res. 26 (7) (2024) 148.
[50] S.O. Jeje, T. Marazani, J.O. Obiko, M.B. Shongwe, Advancing the hydrogen production economy: a comprehensive review of technologies, sustainability, and future prospects, Int. J. Hydrogen Energy 78 (2024) 642–661.
[51] K.J. Kumar, S. Basumatary, J. Daimari, A. Mondal, A.K. Deka, Photocatalytic degradation of methylene blue with polyphenol-rich *Citrus limetta* (peel waste) facilitated ZnO nanoparticles under sunlight, React. Kinet. Mech. Catal. 137 (1) (2024) 483–503.
[52] M. Wasim, A. Mahmood, M. Ashraf, A. Kousar, A. Javed, Surface modification of bacterial cellulose by copper and zinc oxide sputter coating for UV-resistance, antistatic, and antibacterial characteristics, Coatings 10 (4) (2020) 364.
[53] M. Ayuso, J. Sineiro, M. González-Lema, M.Á. Sánchez-Sampedro, P. Corchete, Phenolic composition and biological activities of the *in vitro* cultured endangered *Eryngium viviparum* J. Gay, Ind. Crop. Prod. 148 (2020) 112325.
[54] M.N. Clifford, Chlorogenic acids and other cinnamates – nature, occurrence, dietary burden, absorption, and metabolism, J. Sci. Food Agric. 79 (3) (1999) 362–372.
[55] M. Mesías, et al., Assessment of bioactive compounds, antioxidant capacity, and total browning index during coffee leaves processing, Antioxidants 10 (7) (2021) 1101.
[56] X. Li, et al., Green synthesis of silver nanoparticles using Capsicum annuum L. extract, Green Chem. 13 (8) (2011) 2342–2350.
[57] J. Jeevanandam, et al., Synthesis approaches of zinc oxide nanoparticles: the dilemma of ecotoxicity, J. Photochem. Photobiol. B Biol. 178 (2018) 78–88.
[58] A. Serouti, L.S. Eddine, S. Meneceur, G.G. Hasan, H.A. Mohammed, C. Salmi, K. Iman, M.F. Ferhat, O. Ben Ali, J.A. Abdullah, Biogenic ZnO/CuO/Fe_2O_3 nanocomposite: a groundbreaking approach for enhanced degradation capabilities and reusability in dye removal applications, Arabian J. Sci. Eng. 49 (3) (2023) 753–764.
[59] A. Tabet, S. Meneceur, S.E. Laouini, C. Salmi, H.A. Mohammed, I. Kir, G.G. Hasan, F. Alharthi, J.A. Abdullah, One post biosynthesis of novel ternary nanocomposite ZnO/CuO/Cu_2MgO_3 for enhancing photocatalytic degradation of bromocresol green in wastewater, J. Cluster Sci. 35 (2023) 765–777.
[60] I. Kir, H.A. Mohammed, S.E. Laouini, M. Souhaila, G.G. Hasan, J.A. Abdullah, S.

Mokni, A. Naseef, A. Alsalme, A. Barhoum, Plant extract-mediated synthesis of CuO nanoparticles from lemon peel extract and their modification with polyethylene glycol for enhancing photocatalytic and antioxidant activities, J. Polym. Environ. 32 (4) (2023) 718–734.
[61] M. Azzi, S. Mokni, I. Medila, I. Toumi, G.G. Hasan, S.E. Laouini, M.S. Mahboub, F. Alharthi, F. Menaa, Optimizing synergies: unraveling the effect of ZnO nanoparticle calcination on in vitro antibacterial potency and photocatalytic efficiency of cephalexin—a study into kinetics and isotherms, Chemistry Africa 7 (7) (2024) 3871–3881.
[62] D. Chikushi, Z. Bouaziz, Z. Wang, L. Meng, S. Achour, Biosynthesis of ZnO/Ag nanocomposites heterostructure for efficient photocatalytic degradation of antibiotics and synthetic dyes, Z. Phys. Chem. (2023).
[63] A. Aouadi, D. Hamada Saoud, S.E. Laouini, A. Rebiai, A. Achouri, H.A. Mohammed, A. Bouafia, J.A. Abdullah, F. Alharthi, Synergistic chitin-zinc nanocomposites from shrimp shell waste: characterization, antioxidant, and antibacterial properties, Biomass Conversion and Biorefinery (2023).
[64] S. Ata, W. Zaheer, A. Tabassum, I. Ul Mohsin, I. Altaf, A. ur Rehman, M. Iqbal, Zn/Mn co-doped NiO synthesized by sol-gel route for the photocatalytic degradation of methylene blue dye, ChemistrySelect 8 (37) (2023) e202301940.
[65] F. Ali, A. Ali, G. Mooin Ud Din, U. Younas, A. Nazir, S. Akyürekli, M. Iqbal, W. Mnif, Z. Algarni, Silver and zinc oxide decorated rGO nanocomposites as efficient electrocatalysts towards oxygen evolution reactions under alkaline conditions, Diam. Relat. Mater. 148 (2024) 111378.
[66] T.H. Bokhari, A. Naveed, M.K. Khosa, A. ul Haq, M. Muneer, M. Iqbal, A. Nazir, By-product distribution and cytotoxicity assessment of ZnO-assisted photocatalytic degradation of reactive blue 250 dye, Heliyon 10 (22) (2024) e39670.